

Auger deexcitation of Er³⁺ ions in crystalline Si optically induced by midinfrared illumination

M. Forcales and T. Gregorkiewicz

Van der Waals–Zeeman Institute, University of Amsterdam, Valckenierstraat 65, NL-1018 XE Amsterdam, The Netherlands

M. S. Bresler

A.F. Ioffe Physico-Technical Institute, Politekhnikeskaya 26, St. Petersburg 194021, Russia

(Received 4 April 2003; published 30 July 2003)

We report on the de-excitation of Er³⁺ ions in crystalline silicon, induced by midinfrared radiation from a free electron laser. The effect is interpreted as an Auger energy transfer between excited erbium ions and free holes in the valence band. These are liberated from shallow traps by the powerful mid infrared laser beam. The traps are dynamically populated during the initial band-to-band excitation. The efficiency of the proposed de-excitation mechanism depends on the number of traps occupied at the moment when the free electron laser pulse is applied. Therefore the quenching effect is sensitive to the total number of acceptor traps present in the sample and the excitation density of the pump pulse. A competition between this de-excitation process and the previously reported mid infrared-induced Er photoluminescence enhancement is investigated. The optically induced Auger process, as revealed in this study, complements the description of energy transfer processes in the Si:Er system under optical pumping.

DOI: 10.1103/PhysRevB.68.035213

PACS number(s): 78.66.Db, 61.72.Tt, 41.60.Cr

I. INTRODUCTION

In the last decade, intense research on silicon has been done in order to allow light emission at room temperature. One of the approaches to obtain light out of Si, which has a rather small and indirect band gap, is based on defect engineering.¹ Alternatively, rare earth (RE) doping is used. RE ions are optically active and their atomic transitions cover a wide spectral range. In particular, Er³⁺ is potentially attractive because the energy $\Delta_{ff'}$ of the $4f$ -electron shell transition from the first excited state to the ground state ${}^4I_{13/2} \rightarrow {}^4I_{15/2}$ falls into the interval of minimum losses of silica-based optical fibers used in telecommunication lines.² Recently, we have investigated energy transfers in different RE-doped semiconductors.³ In particular, the role of band gap states in excitation and de-excitation mechanisms of Er³⁺ ions in Si:Er has been studied by means of two-color spectroscopy.⁴ While recombination of an electron-hole pair at an Er-related level (recombination level in the band gap directly linked to erbium) after band-to-band illumination is responsible for Er³⁺ excitation, other levels, not related to erbium, are also involved in energy transfers. Nonequilibrium carriers generated during band-to-band excitation and trapped at defect/impurity levels can be ionized by a midinfrared (MIR) radiation pulse from a free-electron laser (FEL). Using two-color spectroscopy with a FEL we have found enhancement⁵ of Er³⁺ photoluminescence (PL) for temperatures not exceeding 50 K. We have studied this effect in detail⁶ for p -type crystalline Czochralski-grown Si samples with different Er concentrations. The microscopic nature of the MIR-induced PL enhancement has been modelled theoretically⁷ and shown to reproduce satisfactorily the experimental results. Our current investigation reveals that, while the enhancement effect is omnipresent for all investigated Si:Er materials, for some samples also quenching of the Er-related PL occurs upon application of a MIR pulse. We have found that the quenching effect is most pronounced

under conditions of high band-to-band excitation power and with the FEL pulse fired shortly after the primary pump pulse.

In the current study we investigate the nature of the FEL-induced quenching of Er-related PL. We measure the amplitude of the effect at various pumping densities, for different timing and power of the FEL pulse. Upon changing the experimental conditions, we observe a continuous transition between PL quenching and the enhancement effect. We identify the observed PL quenching as being due to an Auger process of energy transfer between an excited state of the Er³⁺ ion and a free carrier ionized into the band by MIR radiation. Based on the experimental results, we propose including this de-excitation mechanism in order to generalize the recently developed model of energy transfers in the Si:Er system.⁷

II. EXPERIMENTAL DETAILS

The experimental data for the present study were obtained for a Si:Er sample prepared from Czochralski-grown p -type silicon. Er ions were implanted with an energy of 300 keV to a dose of $3 \times 10^{12} \text{ cm}^{-2}$. The concentration of erbium in the implanted layer was around $5 \times 10^{17} \text{ cm}^{-3}$. The sample was coimplanted with oxygen ions with an energy of 40 keV to a dose of $3 \times 10^{13} \text{ cm}^{-2}$. Oxygen codoping is known to increase the intensity of Er photoluminescence and to reduce its thermal quenching. The implantation was followed by 1000 °C annealing for 30 minutes. The two-color experiments with a free-electron laser were performed at the “FELIX” users facility in Rijnhuizen (The Netherlands) — for a detailed description of the experimental set up see Ref. 3. In this particular study, excitation densities of the FEL and the Nd:YAG (yttrium aluminum garnet) pump laser were adjusted with internal attenuators and neutral density filters, respectively. A variable delay time between the two pulses was used.

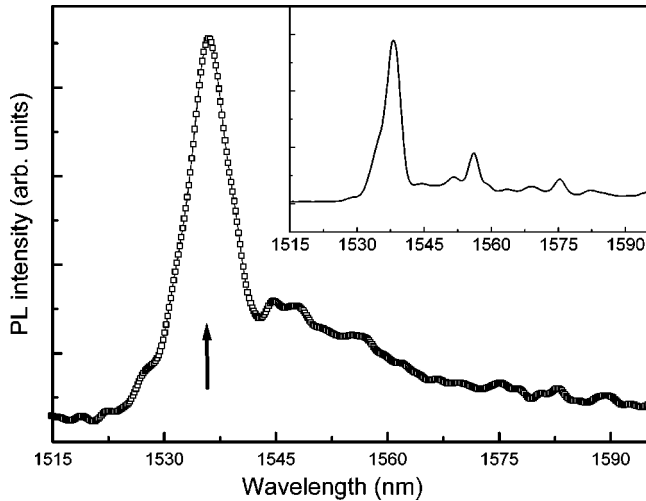


FIG. 1. PL spectrum of the Si:Er at $T=4.2$ K excited with an Ar^+ laser. PL dynamics have been studied for $\lambda=1.537 \mu\text{m}$, as marked by an arrow. In the inset, the PL spectrum of a similar Si:Er sample prepared by identical (Er and O) implantation, but annealed at a lower temperature, is shown for comparison.

III. EXPERIMENTAL RESULTS

In the current research, the spectrum, amplitude, and dynamics of the PL due to transition from the first excited state ($^4I_{13/2}$) to the ground state ($^4I_{15/2}$) of Er^{3+} ions have been investigated at a temperature of $T \approx 5$ K. The PL spectrum obtained from the sample under Ar^+ laser excitation is plotted in Fig. 1. Only a broad peak centered at $1.54 \mu\text{m}$ can be observed here. It is interesting to notice that the identically implanted sample annealed at a different temperature (see the inset to Fig. 1 or Ref. 8,) shows a completely different spectrum indicating a different microscopic structure of optically active Er-related centers. In principle, microscopic information on the optically active Er center can be extracted from a detailed analysis of its PL spectrum. Indeed, it has been shown that Er in crystalline Si can be present in a wide variety of centers.⁹ Unfortunately, in the present case the PL spectrum is very broad, most probably due to inhomogeneity of the sample, and does not allow one to obtain information on the structure of relevant center/s. In Fig. 2 we show the dynamics of the $1.54\text{-}\mu\text{m}$ PL band, marked with an arrow in Fig. 1. PL quenching can be observed upon application of a FEL pulse ($\lambda_{\text{FEL}}=12 \mu\text{m}$, variable power) fired with a delay time of $\Delta t=100 \mu\text{s}$. After the FEL pulse, the PL intensity quenches with a time constant equal to the response time of the experimental set-up ($\tau_{\text{resp}1} \approx 75 \mu\text{s}$) and later decays with the typical Er lifetime of $\tau_{\text{Er}} \approx 1.5$ ms. Using a faster detector ($\tau_{\text{resp}2} \approx 30 \mu\text{s}$, not shown here), the PL quenching still follows the detector response time. We therefore conclude that the quenching process is very fast. In order to quantify the magnitude of PL quenching, we define the quenching ratio Q_R of PL amplitudes as measured with and without the FEL pulse: $Q_R = A_{\text{FEL}}/A_{\text{NoFEL}}$. Naturally, $Q_R = 1$ when the FEL is not applied. While the quenching ratio Q_R is independent of a particular moment when the amplitudes are compared, in experimental practice we should avoid possible errors due to detector response. In particular,

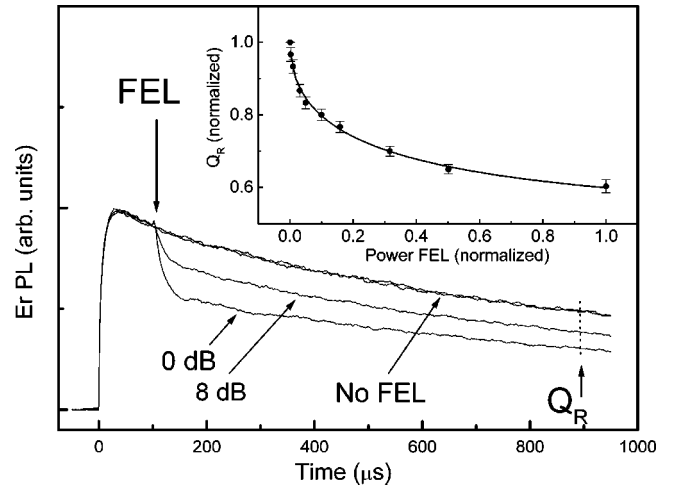


FIG. 2. Dynamics of the Er PL quenching for high Nd:YAG excitation density. The quenching effect is illustrated for a delay time of $100 \mu\text{s}$ and at two energies of the FEL pulse (attenuations 0 and 8 dB). In the inset, the quenching ratio Q_R is shown as a function of the FEL pulse energy.

in Fig. 2 we show Q_R as measured at $t=900 \mu\text{s}$. In the inset to Fig. 2, the quenching ratio is plotted as a function of FEL power. As can be seen, Q_R initially decreases with FEL power (the quenching effect increases), and then saturates. We note that such a behavior is similar to that of the MIR-induced enhancement of Er PL,⁷ thus indicating a possible relation between these two effects.

In order to study the PL quenching further, it would be interesting to investigate the effect as a function of the FEL pulse duration. Unfortunately, this is not possible due to experimental reasons. However, we can move the short Nd:YAG pump pulse ($\Delta t_{\text{YAG}} \approx 0.1$ ns) within the duration of the much longer FEL pulse ($\Delta t_{\text{FEL}} \approx 5 \mu\text{s}$). As can be seen in Fig. 3, no quenching effect is observed when the FEL pulse hits the sample earlier than the band-to-band excitation. This result rules out the possibility that PL quenching takes place as a result of lattice heating due to phonon generation, since thermal effects have relaxation times of milliseconds. In Fig. 3 the quenching effect ($1 - Q_R$) is plotted versus delay time between the Nd:YAG pump pulse and the onset of the FEL pulse. It can be seen that the quenching effect grows linearly during the $5 \mu\text{s}$ of the FEL pulse, with a fairly smooth onset, and later it stops as the FEL pulse terminates. This is a clear indication that the Er PL quenching is related to the “effective duration” of the MIR illumination following the Nd:YAG pump pulse. Consequently, PL quenching appears to be proportional to the number of MIR photons absorbed by excited Er^{3+} ions.

Finally, an important result is given in Fig. 4 which shows the influence of the Nd:YAG power on the quenching effect. The experimental data represent the effect of a FEL pulse ($\lambda_{\text{FEL}}=12.5 \mu\text{m}$, delay time of $\Delta t=500 \mu\text{s}$) at four different pump powers ($P4$ to $P1$). As can be seen, a transition from quenching to enhancement occurs as the pumping density is reduced. A similar transition can also be observed under conditions of high Nd:YAG power, when the FEL de-

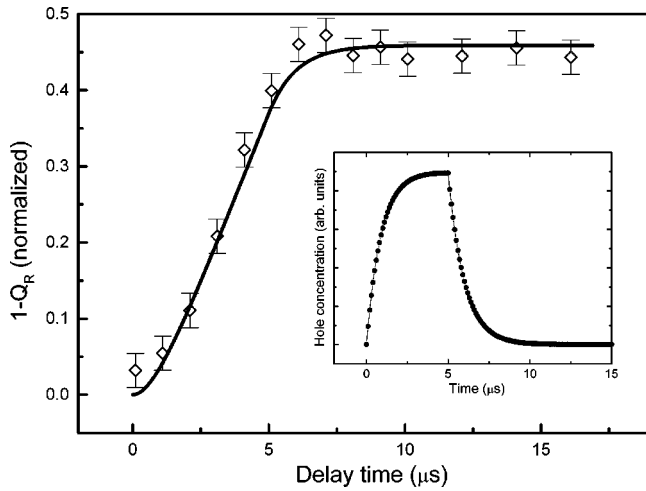


FIG. 3. The quenching effect, defined as $1 - Q_R$, as a function of the delay time between the short Nd:YAG band-to-band excitation and the onset of the longer ($\sim 5 \mu\text{s}$) FEL pulse. The solid line is the numerical simulation based on Eqs. (5) and (6). In the inset, concentration of free holes in the valence band during and after the the ionization pulse of FEL is simulated from the proposed model. See text for further explanation and for the parameters used in the simulation.

lay time Δt is increased from \sim few μs to \sim ms; see the inset to Fig. 4.

IV. DISCUSSION

The experimental evidence presented in Sec. III suggests that the PL quenching and the previously investigated MIR-induced Er PL enhancement are mutually linked, and probably related to the same change of the matrix property induced by the FEL pulse. We conclude that the energy transfer mechanisms activated under the influence of FEL illumina-

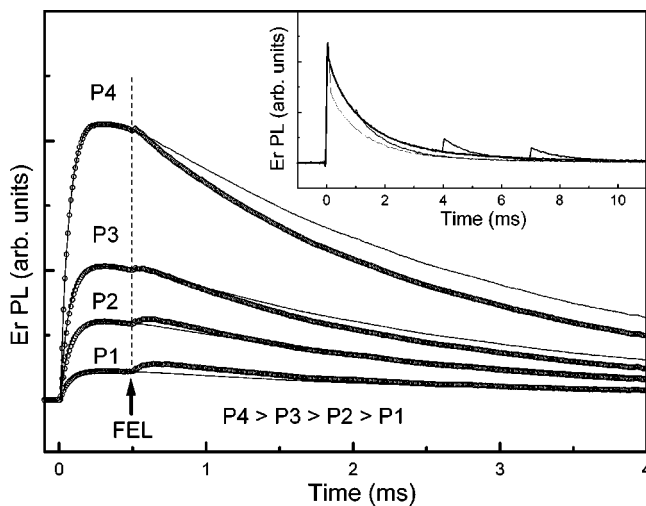


FIG. 4. Dynamics of the Er PL ($\lambda = 1.537$, $T = 4.2$ K) for different Nd:YAG pump excitation density (P4 to P1). The FEL pulse is fired at the delay time of $t_{\text{FEL}} = 500 \mu\text{s}$. A transition from the quenching to the enhancement is observed upon decreasing the Nd:YAG power.

tion depend critically on the available number of excited Er^{3+} ions and carrier traps populated at the moment of the FEL pulse — both being determined by the Nd:YAG pulse energy and the timing of the FEL pulse.

In order to understand the phenomenon responsible for the Er PL quenching induced by MIR radiation, we examine first de-excitation mechanisms identified for Si:Er. Here we can distinguish energy transfers between different erbium ions and between erbium ions and Si. In the later case, Er^{3+} de-excitation by phonon generation or Auger de-excitation induced by free carriers are well known effects.

The exchange of energy between erbium ions in excited states leads to up-conversion,¹⁰ which results in emission quenching. An excited Er ion, de-excites nonradiatively by transferring the energy to another (neighbor) excited Er ion, promoting it into a higher excited state. At this stage, one excited Er^{3+} ion is lost and PL will quench: instead of two excited ions with the probability to emit two photons, only one remains. Relaxation from the higher excited state can be accomplished either by non-radiative transition to the first excited state ($^4I_{13/2}$) from which emission at $1.5 \mu\text{m}$ can follow, or radiatively from higher lying states, e.g., $^4I_{9/2}$ or $^4I_{11/2}$. In this latter case, the relevant photon energy is larger than the band gap of Si ($E_G = 1.17$ eV) and the emitted photon will be absorbed by Si. However, for efficient up-conversion, the concentration of erbium has to be of the order of $\sim 4 \times 10^{20} \text{cm}^{-3}$, which is not the case here. Therefore up-conversion is not considered to be an important mechanism in our Si:Er system, and we resort to energy transfers between Er^{3+} ions and Si.

It is accepted that Er^{3+} introduces a recombination level (of donor character) in the energy band gap of Si. This level is responsible for the energy transfer to the Er^{3+} ion in the excitation process. After band-to-band excitation, electrons are captured at this level and they recombine nonradiatively (in an Auger process) with holes from the valence band. As a result, energy is transferred to the $4f$ -electron shell and Er^{3+} ions attain the excited state. The Er-related level in the gap can be interpreted as an intermediate step necessary for excitation. It was suggested by theory,¹¹ and later supported by experimental work on thermal quenching of PL intensity and lifetime of Er^{3+} ions,¹² that the Er-related level was situated ~ 150 meV below the bottom of the conduction band. It is generally considered that the main process preventing intense emission from Si:Er at room temperature is an efficient non-radiative mechanism called “back-transfer.” In this mechanism, Er^{3+} deexcites and transfers its energy to bring an electron from the valence band to the Er-related level. In that way, the Er excitation mechanism is reversed. The energy mismatch of this process, $(E_G - 150 \text{ meV} - \Delta_{ff'}) \approx 220$ meV, can be provided by phonons generated at higher temperatures. The microscopic model of the back-transfer mechanism was first proposed for InP:Yb (Ref. 13) and later adopted for other RE-doped semiconductors, in particular also for the Si:Er system.¹⁴ In order to investigate this prominent de-excitation mechanism, the FEL can conveniently replace the indiscriminate thermal activation. In the temperature range of this study, $T \approx 5$ K, practically no phonons are available, and the energy necessary for activation of the

back-transfer can be provided optically with photons whose energies fall in the range of the energy mismatch. Indeed, with two-color spectroscopy using MIR radiation, we have observed experimentally the back-transfer process in InP:Yb.¹⁵ Unfortunately, for Si:Er the maximum available energy of the FEL-generated MIR photons is lower than the energy mismatch, $(h\nu)_{max}^{FEL} < 220$ meV, and optical activation of the back-transfer is not to be expected.

Also dissociation of excitons bound to isoelectronic defects formed by Cu and Ag in a Si matrix has been reported to take place under FEL illumination, leading to a quenching of the related PL bands.¹⁶ However, the decrease of the Si:Er PL observed in the present study cannot be explained exclusively by dissociation of excitons. The lifetime of an exciton bound at the Er-related level is of the order of $1 \mu s$,¹⁷ and that of free excitons will not exceed few hundreds of μs ; thus we could not expect quenching at a delay time of $\Delta t = 100 \mu s$, as seen in Fig. 2, or larger. Moreover, as depicted in the inset of Fig. 4, for larger delay times (millisecond scale) Er PL not only shows quenching but also enhancement, which suggests a more complex mechanism.

Taking into account our earlier work on the MIR-induced energy transfers in Si:Er,⁶ we postulate assigning the quenching effect to an Auger de-excitation of Er^{3+} ions, due to the energy transfer to free carriers appearing into the band following optical ionization of traps by the FEL. The existence of such a process has been suggested earlier from investigations of thermal quenching of intensity and lifetime of the Er-related PL in Si.¹² The proposed Auger de-excitation induced optically by MIR radiation complements the model of energy transfers in Si:Er system under optical pumping developed in our earlier studies. In this approach we consider that holes in the valence band, optically released from shallow traps by the FEL pulse, give rise to the simultaneous occurrence of two (independent) processes, of which one leads to excitation and the other to de-excitation of Er^{3+} ions. In that way here we present a model which permits a consistent description of results obtained under various experimental conditions for differently prepared Si:Er materials. It follows from the assumption that the unusual annealing regime of the sample used in the present study results in a high concentration of acceptor traps and partial disordering of the Si matrix. This assumption is supported by a broad, possibly inhomogeneous, line shape of the Er^{3+} PL spectrum, as seen in Fig. 1s. The observed spectrum resembles that of Er^{3+} ions in SiO_2 or in disordered amorphous hydrogenated silicon¹⁸ and is clearly different from that obtained in samples with the usual treatment — see the inset to Fig. 1. The model of the proposed energy transfer mechanisms is schematically depicted in Fig. 5 and, in addition to the Auger quenching, includes the same processes invoked previously in order to explain the afterglow and the MIR-induced Er PL enhancement effects. First, we assume that the system is “prepared” for FEL probing by pumping with a Nd:YAG laser. After band-to-band illumination, the generated free electrons and holes are captured at donor (Er-related level, D_{Er}) and acceptor (boron, A_{tr}) traps, respectively. Slow release of holes from traps (labeled 1) gives rise to the afterglow effect due to recombination with electrons at the

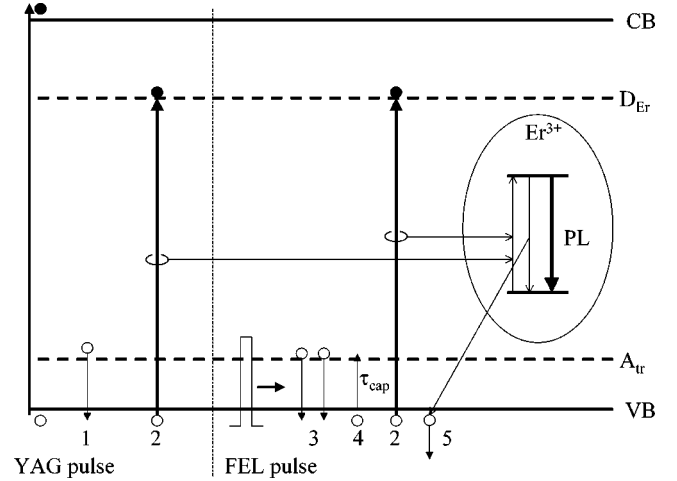


FIG. 5. Schematic illustration of the proposed model of energy transfers. See the text for a detailed explanation.

Er-related center (labeled 2).⁶ During the FEL pulse, holes are released into the valence band (labeled 3). We now consider three possibilities.

(1) Holes can be recaptured at the traps (labeled 4) with a characteristic capture time τ_{cap} .

(2) Holes can recombine nonradiatively with electrons at D_{Er} with a subsequent energy transfer to Er^{3+} ions (the excitation mechanism labeled 2)

(3) Holes can acquire energy from excited Er^{3+} ions leading to quenching of the Er-related PL (labeled 5).

This last mechanism, representing the Auger de-excitation process of Er^{3+} ions by free holes, is a new element introduced into the model.

Since, as discussed earlier, the observed PL quenching takes place on a short time scale of a few μs , in the description of this process we can disregard the release of carriers (labeled 1) giving rise to the afterglow, which is slow at the temperature of the experiment. In that way, for a formal description of the model depicted in Fig. 5 we can propose a set of rate equations valid during the FEL pulse, i.e., for $t \leq 5 \mu s$. In that case the concentration p of free holes in the valence band will be given as

$$\frac{dp}{dt} = \beta I_{FEL} [N_{tr}(t_{FEL}) - p] - \frac{p}{\tau_{cap}}, \quad (1)$$

where β is the MIR radiation absorption coefficient for trap ionization, I_{FEL} is the excitation density of the FEL beam, and $N_{tr}(t_{FEL})$ is the concentration of populated acceptor traps at the time when FEL is fired t_{FEL} . Equation (1) describes how the number of free holes changes due to the release from acceptor traps by a FEL pulse (labeled 3 in Fig. 5) and recapture at the traps (labeled 4 in Fig. 5). $N_{tr}(t)$ is given by

$$N_{tr} = N_{tr}(t_{FEL}) - p, \quad (2)$$

where $N_{tr}(t_{FEL}) = N_{tr}^0 \exp(-t_{FEL}/\tau_{sr})$. Here τ_{sr} is the slow recombination or thermalization time due to release of holes from acceptor traps into the valence band, $\tau_{sr} \approx 30$ ms,⁶ and

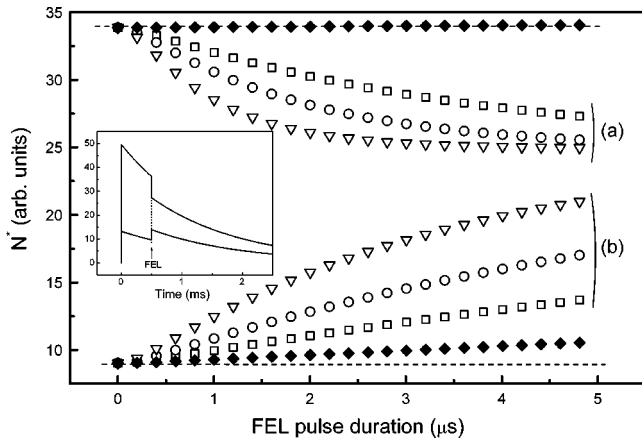


FIG. 6. Simulation based on the proposed model to explain transition from Er PL quenching to enhancement during the FEL pulse. Curves (a) and (b) are for high and low pump powers, respectively. Depending on the concentration of traps and initially populated excited Er³⁺ ions the transition between these two regimes is observed. See the text for further details.

N_{tr}^0 is the concentration of traps initially populated by the pump pulse (note that this value depends on the initial band-to-band excitation density as well as on the total concentration of traps available in the material).

Finally, the concentration of excited Er³⁺ ions, N^* , is described as

$$\frac{dN^*}{dt} = C_{AP}(N_{Er}^{TOTAL} - N^*) - C_{DP}N^* - \frac{N^*}{\tau_{Er}}, \quad (3)$$

where N_{Er}^{TOTAL} is the total concentration of optically active erbium ions, C_A and C_D are the coefficients for the processes of excitation and Auger de-excitation, respectively, and τ_{Er} is the lifetime of erbium in the excited state. The first term in Eq. (3) indicates an excitation of Er³⁺ which leads to the MIR-induced enhancement of Er PL. The second term describes the de-excitation due to the interaction of Er³⁺ ions with free holes, and the last term describes the spontaneous decay of erbium.

Rate equations (1)–(3) can be solved analytically leading to an expression for PL intensity as a function of experimental and material parameters. Here we restrict ourselves to numerical simulations of the above set of rate equations illustrating the evolution of the system. In Fig. 6 we present how the concentration of excited Er³⁺ ions N^* (determining PL intensity) changes during the FEL pulse for two different regimes of (a) high and (b) low powers of the initial band-to-band pump pulse, respectively. The initial population of excited Er³⁺ ions at the beginning of the FEL pulse $N^*(t_{FEL})$ depends on the initial band-to-band excitation density, as well as on the total concentration of Er³⁺ ions and trapping centers N_{Er}^{TOTAL} and N_{tr}^{TOTAL} , respectively, as previously reported.⁶ Indeed, for high pump powers even saturation of the excited erbium and populated traps can be reached. The simulation is performed for $t_{FEL} \approx 500 \mu s$ and is based on the following physical parameters: $\tau_{cap} \approx 0.2 \mu s$, $\tau_{Er} \approx 1.5$ ms, and $C_A/C_D \approx 1$. Keeping these parameters

fixed we set the ratio of $N_{tr}^{TOTAL}/N_{Er}^{TOTAL}$ to 0.04 (squares), 0.09 (circles), and 0.2 (triangles) in order to estimate the importance of the total number of acceptor traps for the observed effects (thus reflecting the unusual heat treatment used for the material investigated, as discussed earlier).

As can be seen from Fig. 6 [curves labeled (a)] and in the inset to the figure, for high band-to-band excitation density (when saturation of both Er excitation and trap population is approached) we observe a reduction of N^* by the end of the FEL pulse. This means that, although enhancement and quenching processes occur simultaneously, the Auger effect prevails and a net decrease of PL intensity is observed. For low excitation density, curves labeled (b), which is the case where many Er³⁺ can still be excited, we see that by the end of the FEL pulse N^* increases, thus leading to an enhancement of the PL signal. In that way we can now understand the experimentally observed transition from quenching to enhancement upon increase of excitation pump density. Naturally, in a similar way we can also explain the same transition occurring while changing the delay time between the pump and the FEL pulses, depicted in the inset to Fig. 4 (although we do not show a simulation of this process). The later the FEL is fired, the more probable it is to observe the net enhancement of PL: since Er³⁺ decays with a lifetime of $\tau_{Er} \approx 1.5$ ms, then when FEL is fired with a delay of $\Delta t = 3$ ms, many Er³⁺ ions will be available for excitation while only a small number of them in the excited state will contribute to the Auger quench. We note that for a fixed pump density and delay time, either an enhancement or a quench will dominate regardless of the power of the FEL pulse; therefore the transition between enhancement and quench can never be observed by varying the FEL power, as indeed confirmed experimentally.

The dependence of the quenching effect on FEL power simulated for a fixed pump density and one delay time ($t_{FEL} \approx 100 \mu s$) is depicted by the solid line in the inset to Fig. 2. It turns out to be similar to the behavior as for the Er PL enhancement,⁷ with the saturation appearing due to a ionization of all the populated acceptor traps. Determination of the absolute values of the physical parameters entering the rate equation set (1)–(3) is difficult. In the simulations in Fig. 6 we have used $C_A/C_D \approx 1$, assuming that the excitation and de-excitation processes are equally efficient, so there is no preference for one specific mechanism. Also we have chosen a range of values from $N_{tr}^{TOTAL}/N_{Er}^{TOTAL} \approx 4\%$ till 20%, anticipating a high concentration of traps which could contribute to the Auger de-excitation. In the previously developed model⁶ the Auger quenching mechanism was not included. This was not necessary, as in that case no quenching of PL was observed regardless of pump power or delay time. In order to account for that experimental evidence we perform a simulation taking a different value of C_A/C_D ratio using the same fixed delay time. This is depicted in Fig. 6 (solid diamonds) for a $N_{tr}^{TOTAL}/N_{Er}^{TOTAL} \approx 1\%$. As can be seen, if $C_A > C_D$ no quenching is observed even for the highest pump power (as was the case for the Si:Er materials investigated in our previous studies), and only the enhancement effect is possible.

A separate issue is the PL quenching dependence on the effective duration of the FEL pulse depicted in Fig. 3 as $(1 - Q_R)$. In order to simulate this effect we simplify the rate equations. If we are in a high band-to-band excitation density regime, N^* saturates to the value N_{Er}^{TOTAL} . As a consequence, the first term on the right side of Eq. (3) becomes zero. During $t < 5 \mu s$, the new Eq. (3) will be

$$\frac{dN^*}{dt} = -C_{DP}N^*, \quad (4)$$

where we have neglected also the term N^*/τ_{Er} , because the duration of the FEL pulse is much shorter than the lifetime of Er^{3+} ion in the excited state $\Delta t_{FEL} \ll \tau_{Er}$ (with this we make an approximation that during the short pulse none of the erbium ions de-excites). For the concentration of free holes in the valence band we take the solution of Eq. (1), as depicted in the inset of Fig. 3 (during and after the FEL pulse). If we introduce this solution into Eq. (4) we obtain that Er PL quenching is proportional to the integrated action of free holes. It can be shown that the evolution of the system is then given as

$$N_{dex} = A \{ \tau_{sr} (1 - e^{-t/\tau_{sr}}) - (\beta I_{FEL} + \tau_{cap}^{-1})^{-1} (1 - e^{-t(\beta I_{FEL} + \tau_{cap}^{-1})}) \} \quad (5)$$

for $t < \Delta t_{FEL}$ and

$$N_{dex} = N_{dex}^0 + p_0 \tau_{cap} \{ 1 - e^{[-(t-t_D)\tau_{cap}^{-1}]} \} \quad (6)$$

for $t > \Delta t_{FEL}$, where N_{dex} is the de-excitation term, defined as $N_{dex} = 1 - (N_{FEL}^*/N_{noFEL}^*)$ and taking the values of $A = \beta I_{FEL} N_{tr}^0 / (\beta I_{FEL} + \tau_{cap}^{-1} - \tau_{sr}^{-1})$, $p_0 = A [e^{-t_D/\tau_{sr}} - e^{-t_D(\beta I_{FEL} + \tau_{cap}^{-1})}]$, and $N_{dex}^0 = A \{ \tau_{sr} (1 - e^{-\Delta t/\tau_{sr}}) - (\beta I_{FEL} + \tau_{cap}^{-1})^{-1} (1 - e^{-\Delta t(\beta I_{FEL} + \tau_{cap}^{-1})}) \}$. The time is counted from the Nd:YAG pulse. In this case the FEL is switched on (I_{FEL}) with a delay time t_D . The value $\Delta t_{FEL} = 5 \mu s$, is the maximum duration of the FEL pulse. The solutions given by Eqs. (5)–(9) are plotted as a solid line in Fig. 3. For small intervals Δt , this expression gives a quadratic dependence on Δt . The quadratic dependence is valid only in the time interval comparable to the capture time τ_{cap} . The quenching process proceeds even after the FEL pulse terminates until free holes disappear from the valence

band. If we include this fact into consideration we get a smooth transition to the constant value regime, as shown by the solid line in Fig. 3 for $\Delta t > 5 \mu s$.

V. CONCLUSIONS

The microscopic mechanism of abrupt quenching of the 1.54- μm PL band observed in some Si:Er samples upon MIR illumination with a FEL has been identified. Detailed experimental investigation and theoretical modeling have shown that this effect appears due to an Auger process of energy transfer between excited Er^{3+} ions and free holes. The holes appear in the valence band as a result of a FEL-induced optical ionization of traps available in the material and populated by the band-to-band pump pulse. Therefore the effect of PL quenching by the FEL is most pronounced in heavily defected Si:Er materials. In that case it is best viewed under experimental conditions of high density of band-to-band excitation (i.e., close to saturation of Er-related PL) and short delay times between Nd:YAG and FEL pulses. Following the results of this study, we propose to supplement the previous model of energy transfers within the crystalline Si:Er system with an additional term corresponding to the newly identified de-excitation mechanism of Er^{3+} ions. The MIR-induced ionization of shallow traps gives rise to the two competing effects of PL enhancement and quenching; which of them prevails depends on sample parameters and on particular conditions of the experiment. We show that simulations based on the mathematical description with the energy transfer model complemented with the Auger quenching term satisfactorily reproduce the experimental results obtained for differently prepared materials.

ACKNOWLEDGMENTS

We gratefully acknowledge the skilful assistance by the FELIX staff, in particular Dr. A.F.G. van der Meer. We would also like to thank Prof. W. Jantsch for providing Si:Er material used in this study. The work was financial supported by the *Stichting voor Fundamenteel Onderzoek der Materie* (FOM) and the *European Research Office* (ERO). The work of M. S. B. was partially funded by *Nederlandse Organisatie voor Wetenschappelijk Onderzoek* (NWO), and grants from Russian Foundation of Basic Research (Grant No 02-02-17631) and from the Russian Ministry of Science and Technology.

¹Wai Lek Ng, M.A. Lourenço, R.M. Gwilliam, S. Ledain, G. Shao, and K.P. Homewood, *Nature* (London) **410**, 192 (2001).

²E. Desurvire, *Phys. Today* **47** (1), 20 (1994).

³M. Forcales, M.A.J. Klik, N.Q. Vinh, I.V. Bradley, J-P.R. Wells, and T. Gregorkiewicz, *J. Lumin.* **94-95**, 243 (2001).

⁴M. Forcales, M.A.J. Klik, N.Q. Vinh, J. Phillips, J-P.R. Wells, and T. Gregorkiewicz, *J. Lumin.* **102-103**, 85 (2003).

⁵T. Gregorkiewicz, D.T.X. Thao, J.M. Langer, H.H.P.Th. Bekman, M.S. Bresler, J. Michel, and L.C. Kimerling, *Phys. Rev. B* **61**, 5369 (2000).

⁶M. Forcales, T. Gregorkiewicz, I.V. Bradley, and J-P.R. Wells, *Phys. Rev. B* **65**, 195208 (2002).

⁷M. Forcales, T. Gregorkiewicz, M.S. Bresler, O.B. Gusev, I.V. Bradley, and J-P.R. Wells, *Phys. Rev. B* **67**, 085303 (2003).

⁸O.B. Gusev, M.S. Bresler, P.E. Pak, I.N. Yassievich, M. Forcales, N.Q. Vinh, and T. Gregorkiewicz, *Phys. Rev. B* **64**, 075302 (2001).

⁹H. Przybylinska, W. Jantsch, Yu. Suprun-Belevitch, M. Stepikhova, L. Palmetshofer, G. Hendorfer, A. Kozanecki, R.J. Wilson, and B.J. Sealy, *Phys. Rev. B* **54**, 2532 (1996).

- ¹⁰W.J. Miniscalco, *J. Lightwave Technol.* **9**, 234 (1991).
- ¹¹I.N. Yassievich and L.C. Kimerling, *Semicond. Sci. Technol.* **8**, 718 (1993).
- ¹²F. Priolo, G. Franzò, S. Coffa, A. Polman, S. Libertino, R. Barklie, and D. Carrey, *J. Appl. Phys.* **78**, 3874 (1995).
- ¹³K. Takahei, A. Taguchi, H. Nakagome, K. Uwai, and P.S. Whitney, *J. Appl. Phys.* **66**, 4941 (1989).
- ¹⁴A. Taguchi and K. Takahei, *J. Appl. Phys.* **83**, 2800 (1998).
- ¹⁵M.A.J. Klik, T. Gregorkiewicz, I.V. Bradley, and J-P.R. Wells, *Phys. Rev. Lett.* **89**, 227401 (2002).
- ¹⁶G. Davies, T. Gregorkiewicz, M. Zafar Iqbal, M. Kleverman, I. C. Lightowers, N.Q. Vinh, and M. Zhu, *Phys. Rev. B* **67**, 235111 (2003).
- ¹⁷J. Palm, F. Gan, B. Zheng, J. Michel, and L.C. Kimerling, *Phys. Rev. B* **54**, 17 603 (1996).
- ¹⁸H. Kühne, G. Weisser, E.I. Terukov, A.N. Kuznetsov, and V.Kh. Kudoyarova, *J. Appl. Phys.* **86**, 896 (1999).